22.01.2021.

THERMOCHROMIC PHASE TRANSITION IN $CuMo_{1-x}W_xO_4$ SOLID SOLUTIONS PROBED BY RESONANT X-RAY EMISSION SPECTROSCOPY AT THE W L_3-EDGE

LATVIJAS UNIVERSITĀTES
CIETVIELU FIZIKAS INSTITŪTS
INSTITUTE OF SOLID STATE PHYSICS
UNIVERSITY OF LATVIA

Inga Pudza[a], Aleksandr Kalinko[a,b], Arturs Cintins[a], Alexei Kuzmin[a]

a EXAFS Lab

b DESY

http://www.dragon.lv/exafs

OUTLINE

- General motivation
  - Structural and optical properties of $CuMoO_4$
  - P-T diagram
  - $CuMo_{1-x}W_xO_4$ solid solutions
- XAS study
- Theoretical XANES calculations
- RXES study
- Summary

MOTIVATION I

M. Wiesmann, et al., J. Solid State Chem. 132 (1997) 88-97.
F. Rodríguez, et al., Phys. Rev. B 61 (2000) 16497.
M. Gaudon et al., Adv. Mater.19 (2007) 3517.
L. Robertson, et al., J. of Materials Chem. C 3 (2015) 2918-2924.
Q. Morelle, et al., Mater. Lett., 253 (2019) 140-143.

M. Wiesmann, et al., J. Solid State Chem. 132 (1997) 88-97.
T. G. Steiner, et al., J. Anal. Chem. 370 (2001) 731.
M. Gaudon, et al., Inorg. Chem. 46 (2007) 10200-10207.
I. Yanase, et al., Ceram. Int. 39 (2013) 2059-2064.
L. Robertson, et al., J. of Materials Chem. C 3 (2015) 2918-2924.
N. Joseph, et al. Applied Materials & Interfaces 12.1 (2019) 1046-1053.

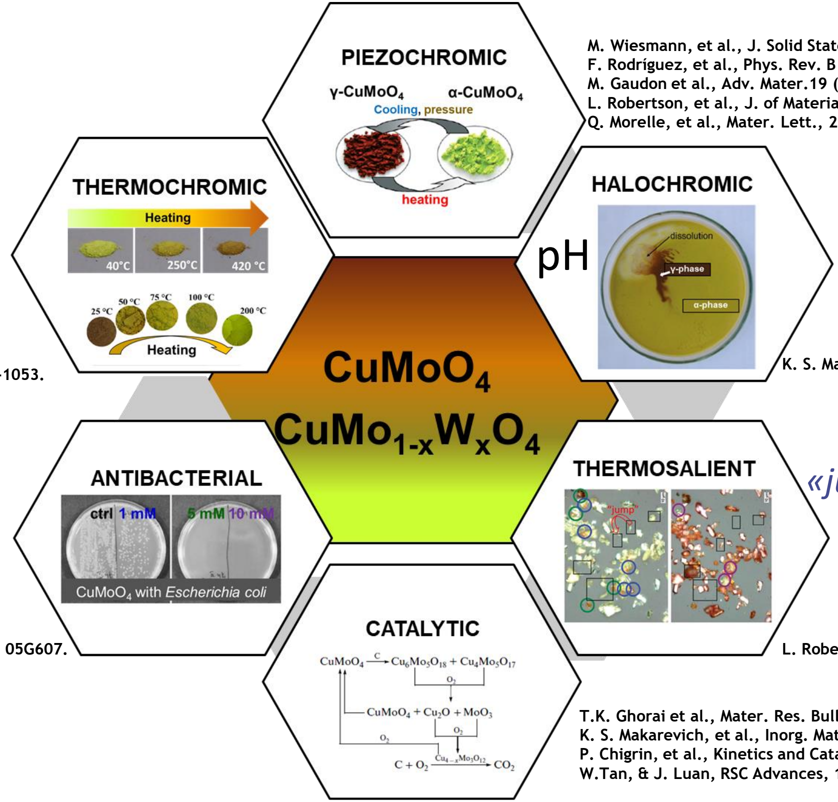

K. S. Makarevich, et al., Inorg. Mater. 46 (2010) 1359-1364.

«jumping crystal effect»

D. Tanasic, et al., Biointerphases 12 (2017) 05G607.

L. Robertson, et al., J. of Materials Chem. C 3 (2015) 2918-2924.

T.K. Ghorai et al., Mater. Res. Bull. 43 (2008) 1770.
K. S. Makarevich, et al., Inorg. Mater. 46 (2010) 1359.
P. Chigrin, et al., Kinetics and Catalysis 54 (2013) 76-80.
W.Tan, & J. Luan, RSC Advances, 10 (2020) 9745-9759.

MOTIVATION II

P-T diagram

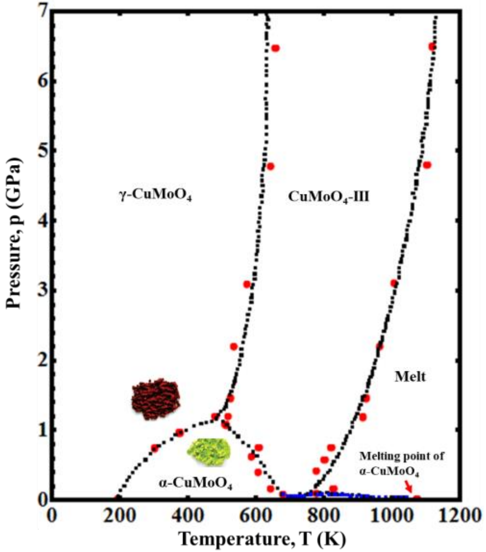

M. Wiesmann, et al., J. Solid State Chem. 132 (1997) 88.

Structure

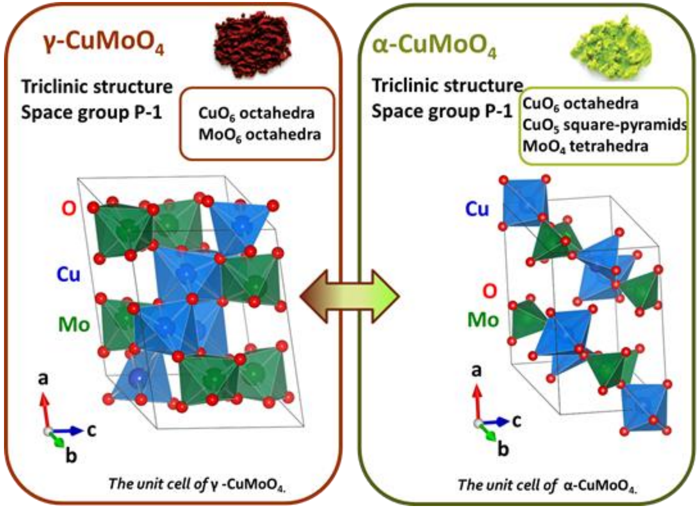

$\Delta V \approx 12 - 13\%$

Hysteresis

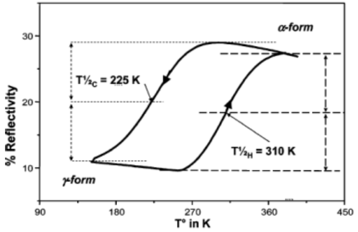

Figure 6. Evolution of the integrated reflectivity percentage in the green zone (500−550 nm) of $CuMo_{0.97}W_{0.03}O_4$ compound with temperature.

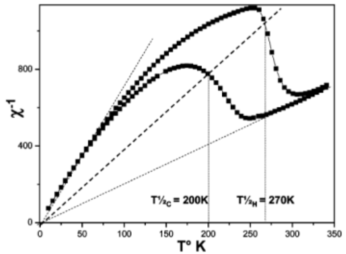

Figure 8. Evolution of the magnetic susceptibility of the $CuMo_{0.95}W_{0.05}O_4$ compound with the temperature.

M. Gaudon, et al., Inorg. Chem. 46 (2007) 10200-10207.
T. Ito, et al., Chem. of Mat., 21 (2009)3376-3379.

MOTIVATION III

The colour

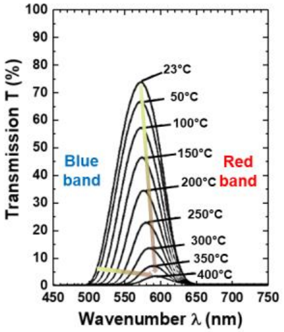

Red shift:

- T ↑
- T ↓
- x ↑
- p ↑

Blue band

$O^{2-} \rightarrow Cu^{2+}$
$O^{2-} \rightarrow Mo^{6+}$
$Cu^{2+} \rightarrow Mo^{6+}$
charge transfer processes

Red band

Cu^{2+} d-d transitions
Cu^{2+} $3d^9 \rightarrow 4p$

T. G. Steiner, et al., J. Anal. Chem. 370 (2001) 731.
F. Rodríguez, et al., Phys. Rev. B 61 (2000) 16497.
M. Gaudon, et al., Inorg. Chem. 46 (2007) 10200-10207.
S. Dey, et al., Inorg. Chem. 53 (2014) 4394-4399.

$CuMo_{1-x}W_xO_4$

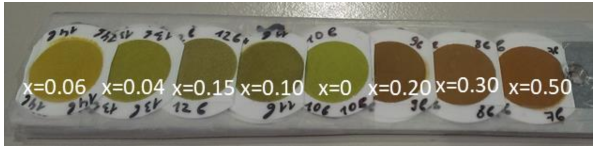

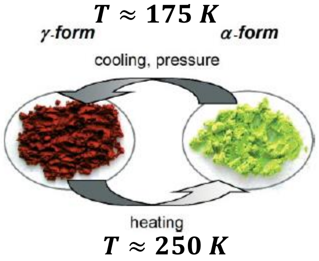

Adaptable thermochromism

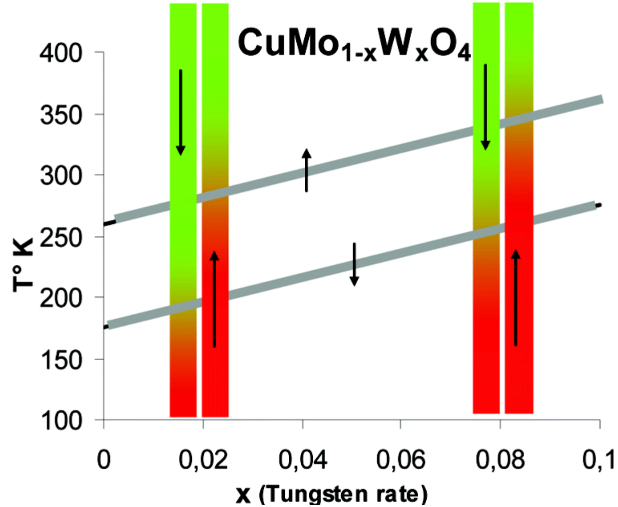

M. Gaudon, et al., Inorg. Chem. 46 (2007) 10200-10207.
X. Wu, et al., Mater. Res. Express 7 (2020) 016309.

XAS STUDY I

PETRA III beamline P65

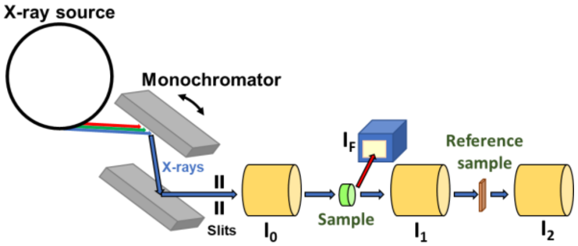

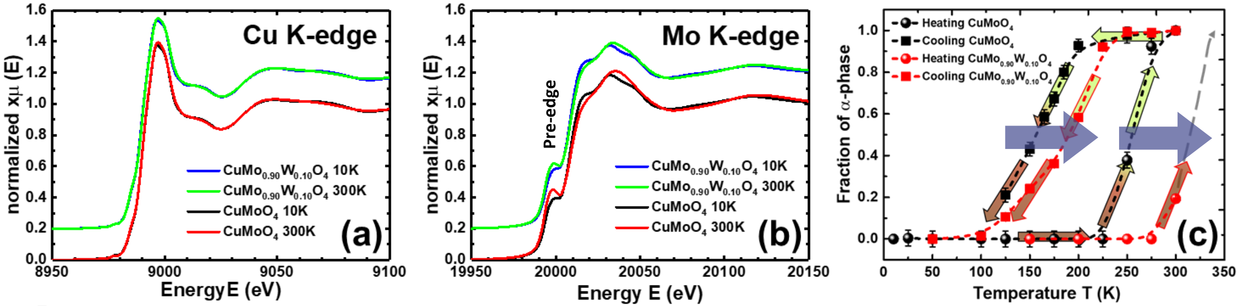

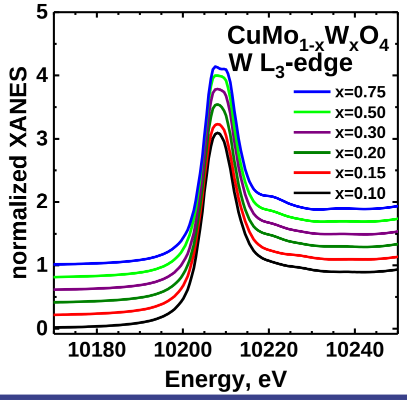

Pre-edge shoulder $1s(Mo) \rightarrow 4d\ (Mo) + 2p\ (O)$

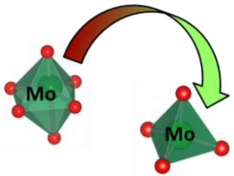

Analysis of the Mo K-edge XANES allows one to reconstruct hysteresis that describes the phase transition.

I. Jonane, A. Cintins, A. Kalinko, R. Chernikov, A. Kuzmin, Low Temp. Phys. 44 (2018) 434-437.
I. Jonane, A. Cintins, A. Kalinko, R. Chernikov, A. Kuzmin, Rad. Phys. Chem. 175 (2020) 108411.

XAS STUDY II

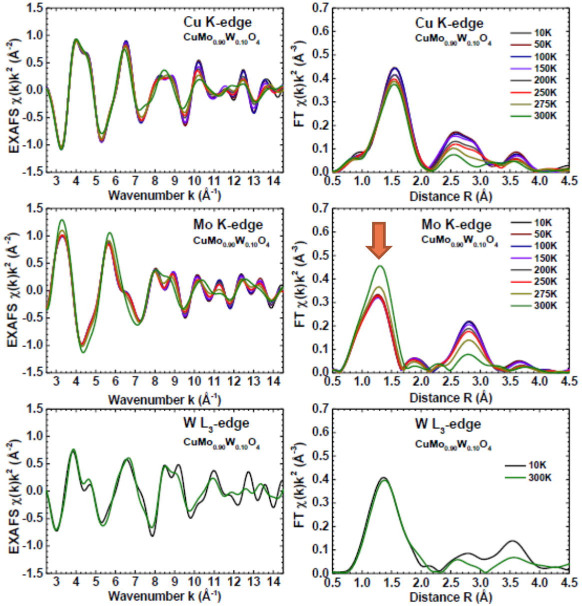

Results from Reverse Monte Carlo (RMC) calculations

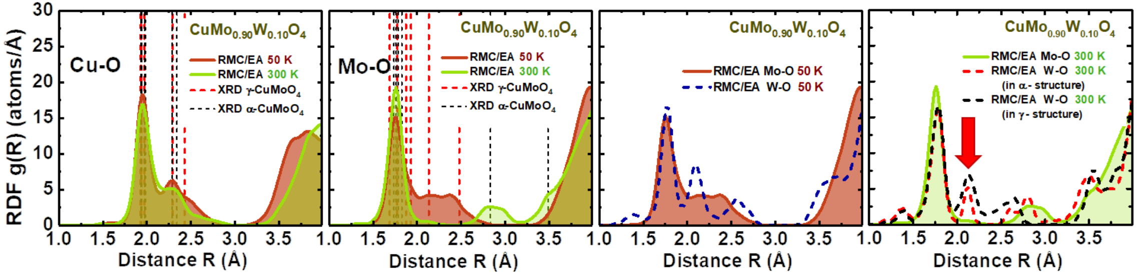

In γ phase W environment is similar to Mo and it is octahedral.
In α phase W tends to have more distorted environment than Mo.

However,
-computationally heavy and time-consuming RMC calculations;
-low content of one of the components;
-the close values of the metal–oxygen interatomic distances.

I. Jonane, A. Cintins, A. Kalinko, R. Chernikov, A. Kuzmin, Low Temp. Phys. 44 (2018) 434-437.
I. Jonane, A. Cintins, A. Kalinko, R. Chernikov, A. Kuzmin , Phys. Stat. Solidi B. 255 (2018) 1800074:1-5.
I. Jonane, A. Anspoks, G. Aquilanti, A. Kuzmin, Acta Mater. 179 (2019) 26-35.
I. Jonane, A. Cintins, A. Kalinko, R. Chernikov, A. Kuzmin, Rad. Phys. Chem. 175 (2020) 108411.

W L_3-EDGE: THEORY VS. EXPERIMENT

Crystal field splitting

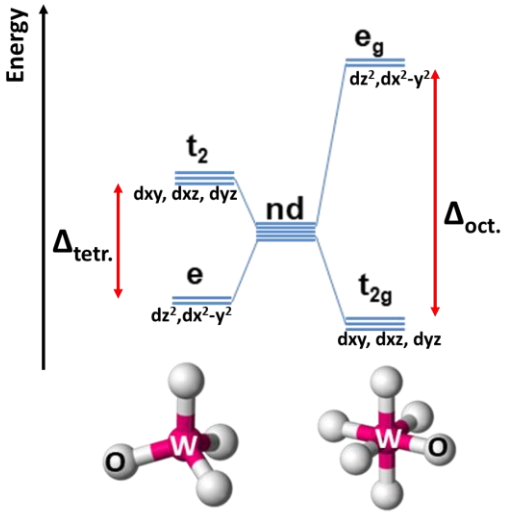

$e:t_2 = 2:3$ $t_{2g}:e_g = 3:2$

FDMNES

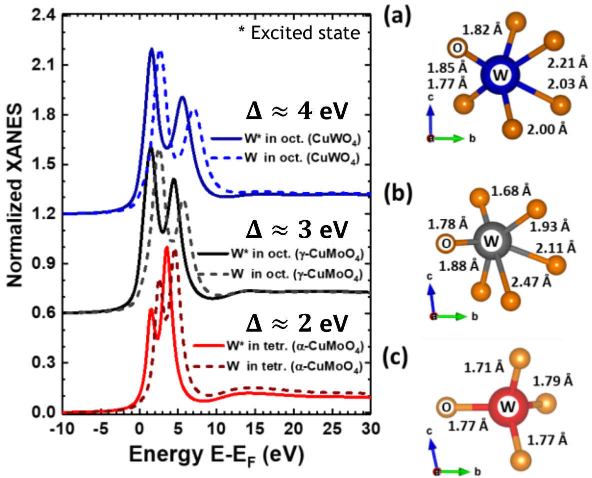

$$\Gamma_{hole} = 1\ eV$$

Experiment

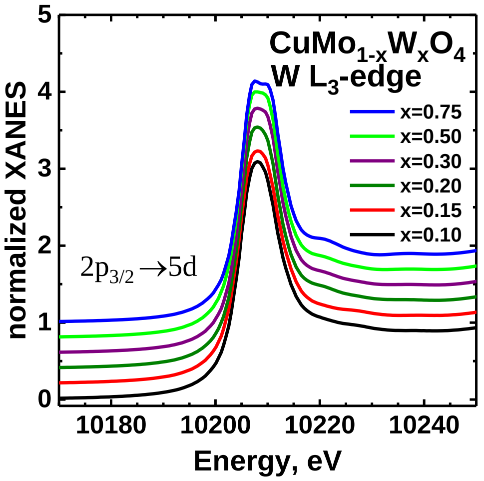

$$2p_{3/2}\ \Gamma_{hole} \approx 4.57\ eV$$

RXES EXPERIMENT

PETRA III P64 Advanced X-ray Absorption Spectroscopy beamline

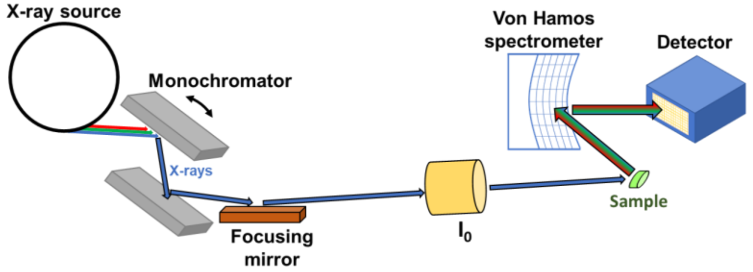

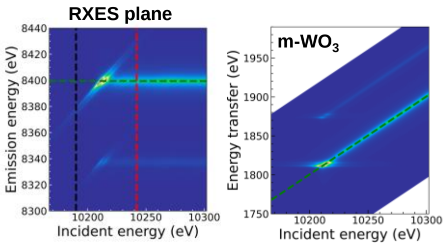

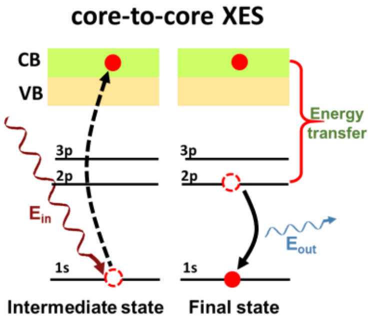

Experimental details:

-High flux ($5 \cdot 10^{11}$photons/s)

-Si(311) monochromator

-100x240 µm focused beam

-Von Hamos-type spectrometer with Si(444) analyzer crystals

-Dectris 2D Pilatus 300 K detector (High-resolution < 1 eV)

-Liquid nitrogen cryostat Linkam THMS600 for low T measurements

W.A. Caliebe, et al., AIP Conf. Proc. 2054 (2019) 060031.
A . Kalinko, et al., J. Synchrotron Rad. 27 (2020) 31-36.

RXES PLANE

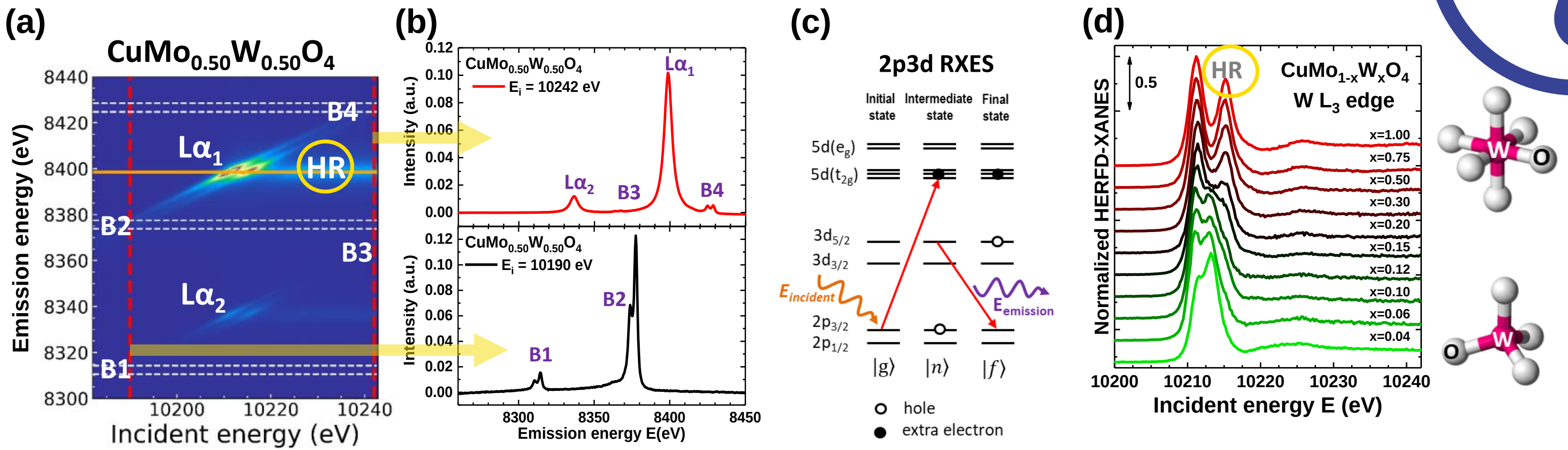

$L\alpha_1$: $3d_{5/2} \rightarrow 2p_{3/2}$

$L\alpha_2$: $3d_{3/2} \rightarrow 2p_{3/2}$

L_3-edge: $2p_{3/2} \rightarrow 5d$

High-energy resolution off-resonant X-ray emission spectra

Below the resonance
$E_i = 10190$ eV

Above the resonance
$E_i = 10242$ eV

High-energy resolution through fluorescence detected XANES (HERFD-XANES)

$E_e = 8398.5 \pm 0.2$ eV

RXES PLANE

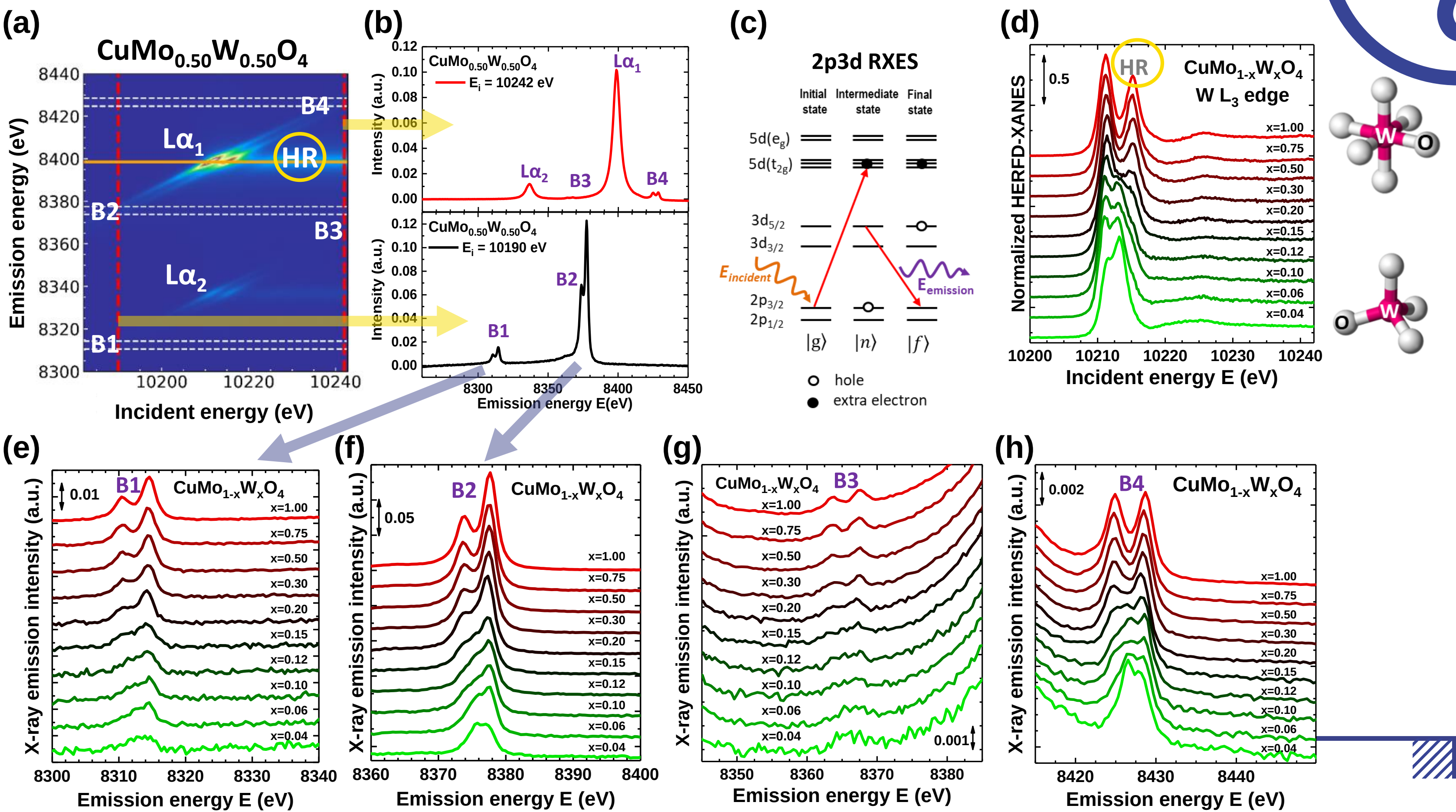

(a)
$CuMo_{0.50}W_{0.50}O_4$
Emission energy (eV)
Incident energy (eV)
B4
Lα1
HR
B2
B3
Lα2
B1
(b)
Intensity (a.u.)
$CuMo_{0.50}W_{0.50}O_4$
E_i = 10242 eV
E_i = 10190 eV
Lα1
Lα2
B3
B4
B2
B1
Emission energy E(eV)
(c)
2p3d RXES
Initial state
Intermediate state
Final state
$5d(e_g)$
$5d(t_{2g})$
$3d_{5/2}$
$3d_{3/2}$
$2p_{3/2}$
$2p_{1/2}$
$E_{incident}$
$E_{emission}$
|g⟩
|n⟩
|f⟩
hole
extra electron
(d)
Normalized HERFD-XANES
HR
$CuMo_{1-x}W_xO_4$
W L_3 edge
Incident energy E (eV)
(e)
(f)
(g)
(h)
X-ray emission intensity (a.u.)
Emission energy E (eV)
$CuMo_{1-x}W_xO_4$
x=1.00
x=0.75
x=0.50
x=0.30
x=0.20
x=0.15
x=0.12
x=0.10
x=0.06
x=0.04

RESULTS – COMPOSITION EFFECT

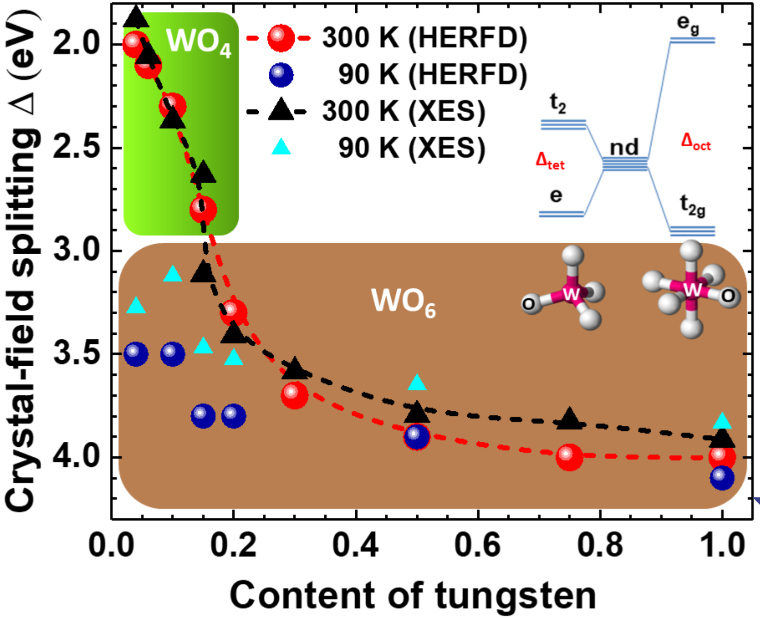

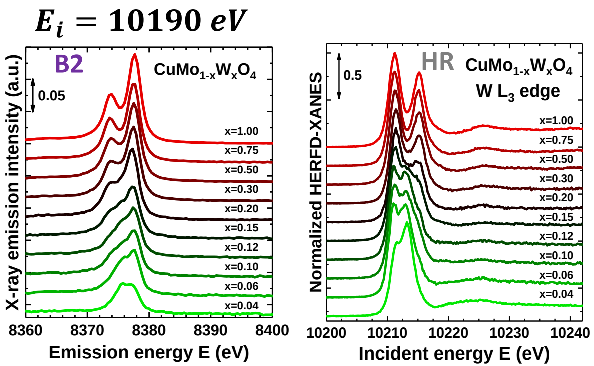

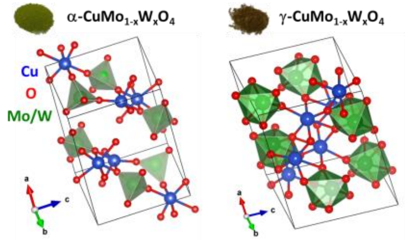

W ions in $CuMo_{1-x}W_xO_4$ solid solutions have octahedral coordination for $x>0.15$ at all temperatures, whereas their coordination changes from tetrahedral to octahedral upon cooling for smaller tungsten content. Nevertheless, some amount of tungsten ions co-exists in the octahedral environment at room temperature for $x<0.15$.

RESULTS – TEMPERATURE EFFECT

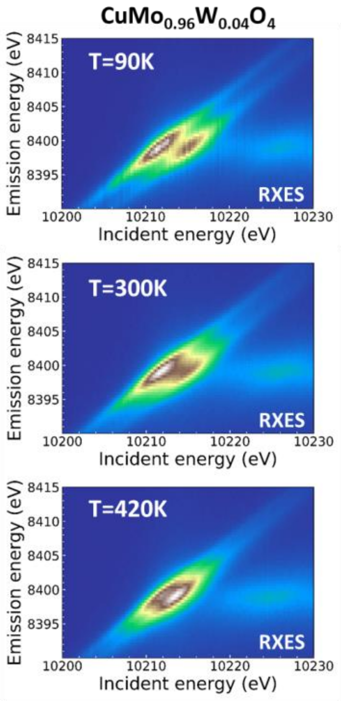

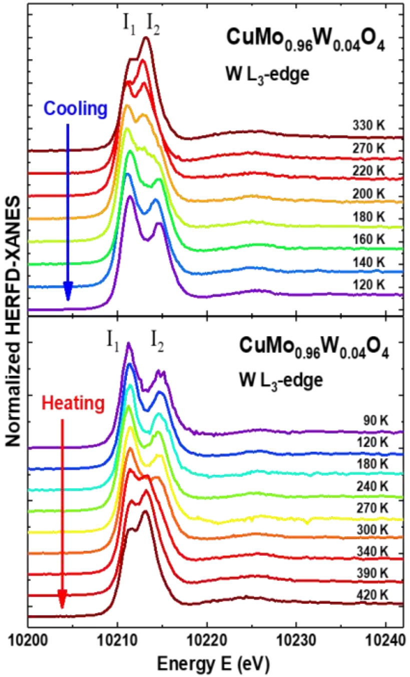

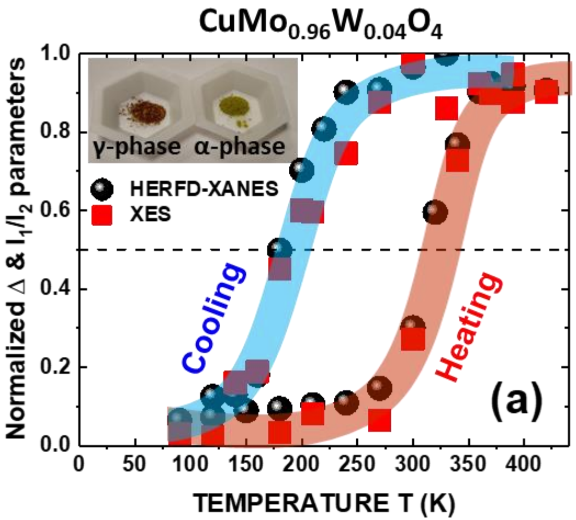

RXES measurements were successfully employed to determine the hysteretic behaviour of the structural phase transition between the α and γ phases in $CuMo_{1-x}W_xO_4$ solid solutions on cooling and heating.

SUMMARY

The analysis of the RXES plane provides useful bulk sensitive information on the coordination of tungsten atoms and allows one to determine the **crystal-field splitting parameter** Δ for the 5d(W)-states.

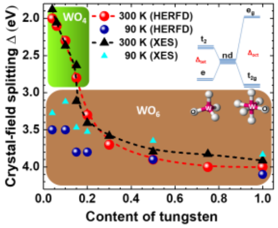

The analysis of the RXES planes shows a clear advantage over conventional XANES due to revealing spectral features with much **higher resolution**.

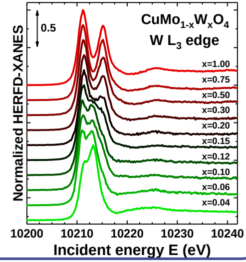

This information can be extracted from the RXES plane by analysing **HERFD-XANES** and the high energy resolution **off-resonant X-ray emission spectra** excited below and above resonance conditions.

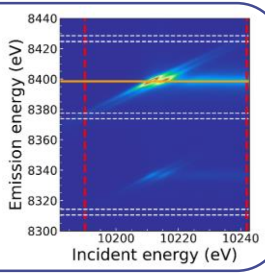

RXES method is well suited for **in-situ measurements** and was used here to determine the hysteretic behaviour of the first-order structural phase transition between α and γ phases in $CuMo_{1-x}W_xO_4$ solid solutions on cooling and heating, even at low (x < 0.10) tungsten content.

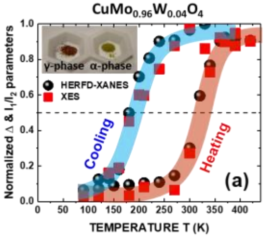

For more details:

I. Pudza, A.Kalinko, A. Cintins, A.Kuzmin, Acta Mater. 205 (2021) 116581.

The financial support provided by the Latvian Council of Science project No. lzp-2019/1-0071 is greatly acknowledged.

FLPP
FUNDAMENTĀLO UN LIETIŠĶO PĒTĪJUMU PROJEKTI

THANK YOU

LATVIJAS UNIVERSITĀTES
CIETVIELU FIZIKAS INSTITŪTS

INSTITUTE OF SOLID STATE PHYSICS
UNIVERSITY OF LATVIA